

J.M. Arblaster · G.A. Meehl · A.M. Moore

Interdecadal modulation of Australian rainfall

Received: 10 December 2000 / Accepted: 14 July 2001 / Published online: 4 January 2002
© Springer-Verlag 2002

Abstract Interdecadal variability is investigated in a 300 year run of the Parallel Climate Model, a global coupled atmosphere-land-ocean-sea ice model. The model simulates El Niño variability of realistic magnitude and is found to produce interdecadal characteristics similar to those observed, both in frequency, spatial patterns and amplitude. Modulation of Australian rainfall on interdecadal time scales is similar to observed and is found to have contributions from both the modulation of ENSO, changes in the position of the Walker circulation and variations in western Pacific SSTs. A slackening of the equatorial Pacific thermocline slope is associated with diminished ENSO variability during interdecadal periods of positive tropical Pacific SSTs. These interdecadal changes to ENSO and shifts in the position of the Walker circulation are physical mechanisms that contribute to the weakened correlations between the SOI and Australian climate during interdecadal periods of positive tropical Pacific SSTs. Warm anomalies in the western Pacific also contribute to a decrease in Australian rainfall in the model on interdecadal time scales.

Niña, or cool event, and positive SOI. However, the recent El Niño of 1997/1998, the strongest El Niño on record (in terms of SST anomaly in the Niño-3 region of the eastern Pacific), did not result in severe drought in Australia. In fact Australian rainfall in 1997 was generally above normal with small-scale weather systems providing much of the precipitation (Walland 1998). An unexpected response to the recent El Niño was also recorded in other regions of the globe *e.g.*, the monsoon rains over India were forecast to be deficient but were also above average (Webster and Palmer 1997).

Recent studies have noted a changing relationship between the El Niño Southern Oscillation (ENSO) and Australian climate. Nicholls et al. (1996) found that the relationship between SOI and Australian rainfall has diminished in the last two decades and suggest that the corresponding warming of the Indian Ocean could result in rainfall modulations as important to Australian climate as ENSO.

Other studies have investigated the influence of interdecadal variability on Australian climate. Latif et al. (1997) noted the strong relationship between an index of Pacific decadal variability and the Australian summer monsoon, with positive phases (above normal tropical Pacific SSTs) of the decadal index resulting in below normal Australian monsoon rainfall. Negative decadal phases (below normal tropical Pacific SSTs) were found to result in above normal monsoon rainfall. Power et al. (1999a) found an interdecadal modulation of the relationship between ENSO and Australian climate. Their index of interdecadal variability, which they name the InterDecadal Pacific Oscillation (IPO) is shown to strongly modulate the correlations of SOI and Australian continental climate variables such as rainfall, maximum temperature, river flow and crop yield. During positive IPO phases, when tropical Pacific SSTs are warmer than average, correlations between SOI and Australian climate are very weak. During negative IPO phases, the correlations are strong.

1 Introduction

Droughts in Australia are often associated with an El Niño, or warm event, in the tropical Pacific, usually indicated by a large negative Southern Oscillation Index (SOI) value. Flooding is often associated with a La

J.M. Arblaster (✉) · G.A. Meehl
National Center for Atmospheric Research,
PO Box 300 Boulder, Colorado, 80307-3000, USA
E-mail: jma@ucar.edu

A.M. Moore
Program in Atmospheric and Oceanic Sciences,
University of Colorado, USA

Interdecadal scale variability is increasingly seen as an important mode of variability in the climate system. Many studies have noted the abrupt change in the global pattern of sea surface temperatures (SSTs) since the early-mid 1970 s, with an ENSO-like warming of tropical Pacific SSTs and cooling in the North Pacific (*e.g.*, Trenberth and Hurrell 1994; Zhang et al. 1997). This change is seen as a natural fluctuation of the climate system. Other abrupt changes occurred during the 1920s and 1940s (Mantua et al. 1997), however the recent regime shift has received the most attention due to the availability of more data in the later period.

Interdecadal variability is found in both the tropical and mid-latitude regions of the Pacific. Both internal and external (*e.g.*, fluctuations in solar insolation) forcing could lead to fluctuations on these time scales. Coupling between the atmosphere and ocean could be important for tropical Pacific decadal variability while in the mid-latitudes both thermohaline and wind-driven effects may be important (Latif 1998). Interaction between the tropics and mid-latitudes on interdecadal time scales has also been hypothesized (Gu and Philander 1997) with Meehl et al. (1998) suggesting interaction that extends to all ocean basins. The mechanism for interdecadal variability in the observations as well as coupled models is beyond our scope here and will be addressed in a subsequent study.

Observational studies suggest that interannual variability in the tropics is modulated on interdecadal time scales. For example, Torrence and Webster (1999) found the variance in Niño-3 SSTs (a measure of ENSO) to decrease substantially during the periods 1920-1960 when compared to the periods 1875-1920 and 1960-1990. Power et al. (1999a) also found that the variance of the SOI was over twice as large during negative phases of the IPO compared to the SOI variance during positive phases of the IPO. The physical processes driving this modulation are unclear. Many studies have suggested an interaction between the north Pacific gyre and the tropical Pacific. Connection through the atmosphere is achieved by variations of the trade winds through mid-latitude SST forcing (*e.g.*, Pierce et al. 2000). The tropical Pacific is very sensitive to changes in wind stress, and long term changes in the tropical winds could influence shorter time scales such as ENSO by modulating the long term east-west slope of the upper ocean. Interactions via the ocean have also been investigated (*e.g.*, Lysne et al. 1997; Gu and Philander 1997) with subsurface anomalies travelling from the mid-latitudes to the tropics where they change the thermocline structure and upwell to the surface. The atmosphere then reacts to these changes in tropical SSTs creating anomalous SSTs of the opposite sign in the mid-latitudes, and the cycle repeats. Other studies have suggested variations of these interactions, however, the physical mechanism responsible for interdecadal modulation of ENSO has not yet been clearly demonstrated and will not be addressed here.

The purpose of this study is to use a global coupled climate model, the Parallel Climate Model (PCM; see Washington et al. 2000), to investigate the interdecadal modulation of Australian rainfall. Modulation of interannual teleconnections, that link variability of SSTs in the tropical Pacific associated with ENSO to Australian rainfall, will be investigated. Sensitivity studies, where the atmospheric component is forced by boundary conditions of observed SSTs and sea-ice concentrations, are used to investigate the influence of the western Pacific on Australia and to gain further insight into the coupled model simulation. Section 2 describes the model and its mean climate simulation. Section 3 evaluates the PCM's ENSO-like variability and links to Australian rainfall. Section 4 examines the interdecadal variability in the PCM and its modulation of Australian climate and Section 5 addresses some possible mechanisms of this interdecadal modulation.

2 Model description

The PCM couples together component models of the land surface, atmosphere, ocean and sea-ice into a fully coupled model of the global climate and is designed to run on the latest technology in supercomputing, the massively parallel computing environments (Washington et al. 2000). A flux coupler is used to exchange surface fluxes at the *e.g.*, ocean-atmosphere interface and also performs the task of interpolating between the different resolutions and grid structures of the component models (Washington et al. 2000).

The atmospheric component of the PCM is the National Center for Atmospheric Research (NCAR) Community Climate Model version 3 (CCM3), which also incorporates the NCAR land surface model (LSM). The CCM3 has a horizontal resolution of T42 (~2.9° grid spacing) and 18 vertical levels. It includes the deep convection scheme of Zhang and McFarlane (1995) and the shallow convection scheme of Hack (1994). Cloud properties are diagnostic. See Kiehl et al. (1998) and Bonan (1998) for further details of the atmospheric component.

The oceanic component of the PCM is the Parallel Ocean Program (POP) model developed at Los Alamos National Laboratory (Smith et al. 1995). The resulting average resolution is 2/3° with increased latitudinal resolution near the equator to 1/2°, which is equivalent to approximately 55 km. The free surface technique and surface pressure formulation used in POP avoids the topographic smoothing required in models with a rigid lid approximation, thus allowing for an unlimited number of land masses and unsmoothed bottom topography (Semtner 1995). The POP model is a descendent of the Bryan and Cox (1967) ocean model which is based on the primitive equations of motion. The vertical diffusion parameterization of Pacanowski and Philander (1991) has been implemented in this version of POP (Washington et al. 2000).

A version of the sea-ice model of Zhang and Hibler (1997) has been optimized for the parallel computing environment required for the PCM. This model has a constant resolution of 27 km and provides realistic sea-ice motion. It uses Zhang and Hibler (1997) sea-ice dynamics with viscous-plastic ice rheology.

The simulation examined here is a 300-year control run with constant 1990 values of greenhouse gases (*e.g.*, CO₂ concentration is fixed at 355 ppm). To spin-up the coupled model the atmospheric component was first forced with observed SSTs and sea-ice concentrations for 10 years. The ocean and sea-ice components were then repeatedly forced with the last 5 years of this atmosphere-only run for a period of 86 years, with acceleration (Bryan 1984) employed in the deep ocean. At this point the fully coupled run is begun. Final adjustments were made to the model

code in year 48 of the simulation so model years 49-348 are examined here. The PCM does not employ flux adjustment. Further details of the spin-up technique can be found in Washington et al. (2000) and Boville and Gent (1998).

Figure 1 shows a comparison of the PCM long term annual mean tropical temperature and precipitation, along with observational estimates. Most features of the mean climate are well represented by the model, including the western Pacific warm pool and the eastern Pacific cold tongue, the InterTropical Convergence Zone (ITCZ) at approximately 10°N and precipitation maximum over South Asia. However, the cold tongue is too narrow and extends too far west and although the model reproduces the slope of the equatorial temperature gradient across the Pacific, the equatorial Pacific waters are a few degrees cooler than observed, a common problem in many models (AchutaRao et al. 2000). The SSTs off the west coasts of South America and Africa are too warm. This is a systematic error in coupled models and could be caused by poor simulation of stratus clouds in these regions (Ma et al. 1996). A double ITCZ, another typical systematic error of coupled models (Meehl and Arblaster 1998), is found at 10°S in the Pacific and the equatorial region is too dry. However, the general structure of the observed tropical climate is captured by the model.

3 ENSO simulation and teleconnections

Meehl et al. (2001) examined the ENSO simulations of several coupled models, including the PCM. In their Fig. 9, the ENSO-like pattern for the PCM was seen to have similar characteristics to the observed El Niño pattern, *i.e.*, warm waters in the tropical Pacific and cool waters in the North and South Pacific. However the warm tropical waters extend too far west in the model shifting the anomalous subsidence during an El Niño over Southeast Asia and Australia further to the west. This westward extension could also contribute to the colder than observed SSTs in the east Indian Ocean.

An index of ENSO is produced by averaging the SSTs over the Niño-3 region (5°N-5°S, 150°W-90°W) in the central to eastern Pacific, indicative of ENSO variability. Meehl et al. (2001) found that the standard deviation of the PCM Niño-3 monthly anomalies (smoothed with a 5-month boxcar smoother, after Trenberth 1997) is 0.90 °C compared to an observed value of 0.86 °C (1950-1998; Reynolds and Smith 1994). This is an indication that the model is simulating eastern Pacific SST fluctuations on the ENSO time scale of realistic magnitude.

In the observations, El Niño events occur every two to seven years with varying strength and frequency and last between twelve and eighteen months (McPhaden et al. 1998). The frequency of El Niño events in the PCM is closer to three to four years, as discussed in Meehl et al. (2001).

A cursory look at the ENSO mechanism operating in the PCM suggests that eastward propagation of thermocline depth anomalies (or upper ocean heat content) generates the SST anomalies in the eastern Pacific, similar to the delayed-oscillator mechanism (McCreary 1983; McCreary and Anderson 1984; Battisti and Hirst 1989; Suarez and Schopf 1988). This mechanism has received much attention and appeared to be operating during the El Niño event of 1997/98 (Webster and Palmer 1997; McPhaden 1999).

Statistical analyses of observations show a strong correlation (~ -0.5) between the Indian monsoon (measured by area averaged rainfall over India) and ENSO such that when an El Niño event occurs in the eastern Pacific the monsoon is usually weaker than normal (Torrence and Webster 1999; Webster et al. 1998). The opposite occurs in a La Niña event. A similar relationship between Australian rainfall and ENSO occurs in the observations (Meehl and Arblaster, 1998; Webster et al. 1998). The correlation between an Australian rainfall index (110°-155°E, 40°S-10°S) and Niño-3 SSTs on annual time scales in the PCM is -0.5 . Hence the PCM is capturing the observed relationship between fluctuations in the eastern Pacific and Australian rainfall. To further illustrate this point, Fig. 2 shows the correlation between annual mean values of the SOI and precipitation at all grid points for the PCM and observations (Xie and Arkin 1996, Reynolds and Smith 1994). During an El Niño, or warm event (where the SOI is negative, and eastern Pacific SSTs are anomalously warm), precipitation shifts east in both the PCM and observations, and the Australian continent is dry due to subsidence there. In the PCM anomalous subsidence extends farther west into the Indian Ocean.

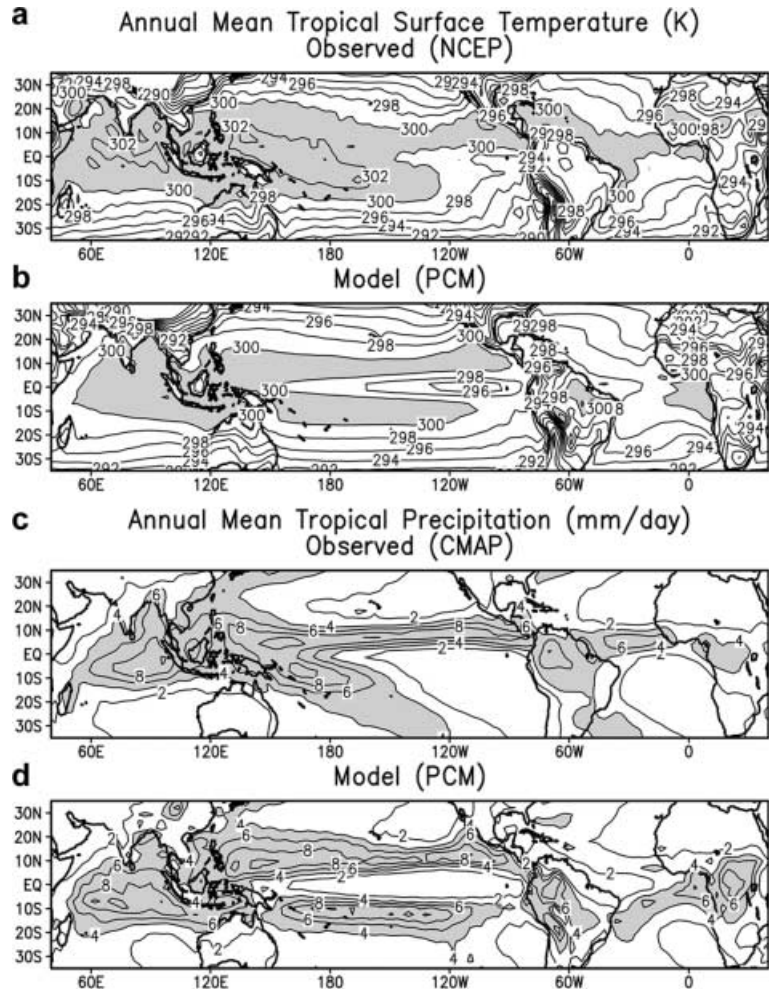
4 Interdecadal variability

The interdecadal variability in the climate system of interest here is manifest as an ENSO-like pattern of SSTs. Folland et al. (1999), in an observational study of near-global SSTs, showed the interdecadal mode of SSTs in their Fig. 4.4f and g which were reproduced by Power et al. (1999a). The interdecadal pattern of the PCM was computed in a similar way to the observed study. Seasonal SSTs from 300 years of the control simulation were low-pass filtered (using a Lanczos filter) with a cut-off of 13 years. The region of the EOF was restricted to 40°S-60°N in an attempt to roughly imitate the mask (due to sparsity of data) used in the observational study of Folland et al. (1999).

4.1 Interdecadal Pacific Oscillation pattern and index

The spatial pattern of the positive phase of the interdecadal mode for the PCM can be seen in the top panel of Fig. 3, the pattern of the first EOF of lowpass filtered seasonal SSTs. This figure is created by correlating the principal component time series from the EOF analysis with the lowpass filtered SSTs at each grid point. As in the observations, there are similarities to ENSO with warming in the tropics and cooling in the north and south Pacific. The warming extends farther into the western tropical Pacific in the interdecadal pattern compared to the ENSO pattern. Furthermore, the magnitude of the anomalies in the northern Pacific are of a similar strength to those in the tropical eastern Pacific, in comparison to ENSO which is dominated by the

Fig. 1 Annual mean tropical surface temperature (*top*) and precipitation (*bottom*) for **a, c** the observations (NCEP/NCAR Reanalyses and CMAP precipitation from 1979-1997;) and **b, d** model (PCM - 200 years). Values above 300K and 4 mm/day are shaded



tropics (similar to Folland et al. 1999). In the interdecadal pattern, greater variance is found in the tropical SSTs of the western Pacific than the eastern Pacific, whereas ENSO is dominated by variance in eastern Pacific SSTs (Latif et al. 1997). Similar percent variances are explained by the interdecadal modes; 15% for the PCM and 13% for the observations. Hence it appears that the model exhibits similar interdecadal variability to that found in the observations.

The lower panel of Fig. 3 is the principal component (PC) time series corresponding to the EOF analysis. Power et al. (1999a) called the observed PC time series their Interdecadal Pacific Oscillation (IPO) index as it represents the dominant mode of variability of near-global (but dominated by Pacific) SSTs on interdecadal time scales. Fluctuations in this time series from positive to negative modes would be expected to cause climate fluctuations in many regions of the globe.

Note that the interdecadal variability in the observational study is captured by the third EOF (Folland et al. 1998). Since external forcing is constant in the PCM control run, the model output does not include the same trend in global temperatures as in the observations. Thus the IPO is the strongest mode of low frequency variability in the run and is therefore the first

EOF. Similar analysis of a twentieth century run of the PCM, with observed greenhouse and sulfate aerosol forcing, results in the interdecadal pattern being the third EOF. The use of the control run here allows a longer time series to be analyzed.

4.2 IPO and mean Australian rainfall

The influence of interdecadal variability on Australian rainfall is evident in the time series' of Fig. 4. The top panel is from Latif et al. (1997) and shows the observed out of phase relationship between their decadal principal oscillation pattern (POP) mode of tropical Pacific SSTs (dotted) and low pass filtered northeastern Australian summer rainfall (solid). The two time series are highly anti-correlated for a 42 year period from 1949-1991 at a value of -0.8 , such that warm (cold) Pacific SSTs on decadal time scales are associated with suppressed (enhanced) NE Australian rainfall. The bottom panel of Fig. 4 shows the same relationship for the model for the 300 year period of the control run. Here, annual Australian rainfall is calculated as an area average over the Australian continent (40°S - 10°S , 110° - 155°E , land points only), similar to Power et al. (1999a), and lowpass

filtered as previously described. The interdecadal index is the IPO index from Fig. 3b. Note the similar out of phase relationship in the model results, with a correlation coefficient of -0.5 . Although the model correlation is less than observed, the model time series is six times longer than the observed record and is thus more statistically significant than the observations.

4.3 Interdecadal modulation of ENSO teleconnections to Australia

Now that we have established that Australian precipitation is modulated on interdecadal time scales in the model, similar to the observations, the next step is to determine whether this modulation is, in part, due to

Fig. 2 Correlation of SOI with precipitation at all grid points, on annual time scales for the **a** observations (Xie and Arkin 1996) and **b** PCM. Values greater than 0.3 are shaded

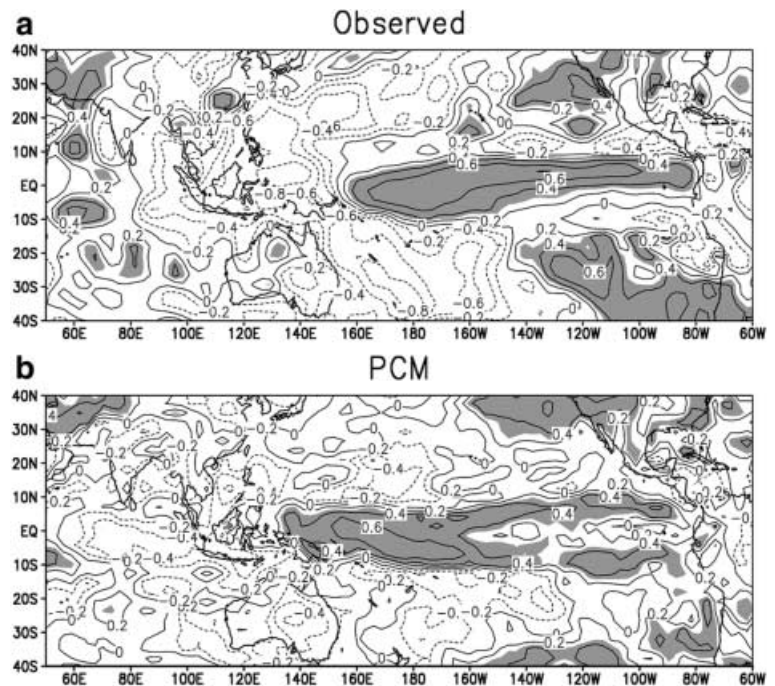
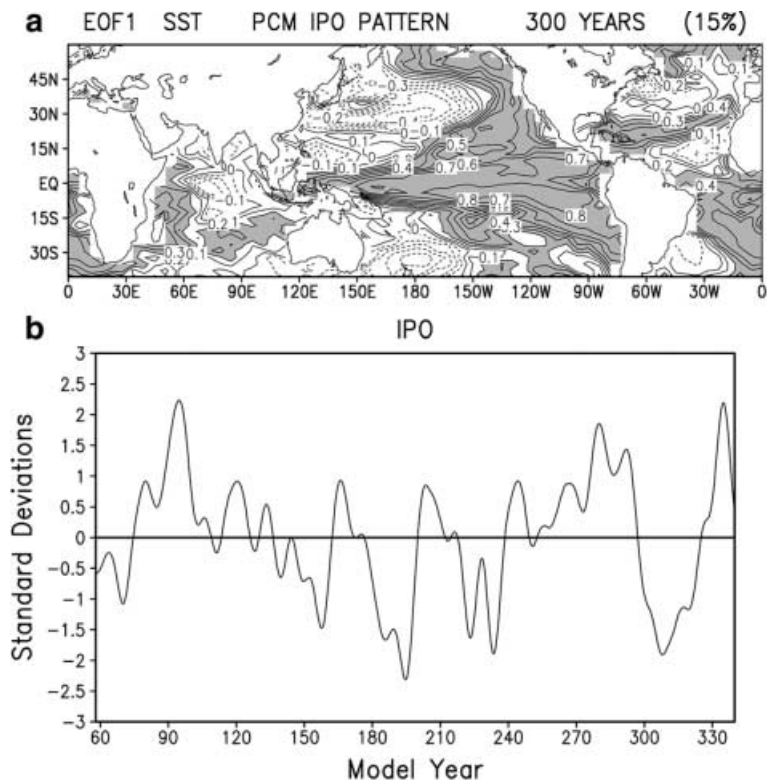


Fig. 3a, b Interdecadal pattern of the PCM calculated as the first EOF of low pass filtered SSTs for the 300 year control run **a** spatial pattern of the positive interdecadal phase, **b** the principal component time series (IPO) in units of standard deviations. The percent variance explained by this mode is given in *parentheses* in the *top right corner*. Values above 0.2 are shaded



interdecadal changes in the interannual relationship between ENSO and Australian climate. An El Niño or warm event in the tropical Pacific is expected to be associated with decreased rainfall in Australia, while a La Niña or cold event is expected to be associated with excess rainfall (Ropelewski and Halpert 1996). Power et al. (1999a) found that these interannual relationships were modulated quite remarkably on interdecadal time scales. Their results are summarized in their Fig. 4 reproduced here in Fig. 5a. Thin lines are correlations between Australian climate indices such as rainfall and temperature with SOI in 13 year running blocks. The thick line depicts the observed IPO index from Folland et al. (1998). From the figure it is clear that strong interannual correlations are found when the IPO is negative and weak correlations when the IPO is positive. Hence, ENSO appears to have a strong influence on Australian climate during periods of negative tropical Pacific SST anomalies on interdecadal time scales, but not during positive interdecadal periods.

Figure 4 from Power et al. (1999a) was recalculated for the model and is shown in Fig. 5b. Attempts were made to exactly duplicate the methods of Power et al. (1999a) for the model. Correlations (in 13 year running blocks) of annual Australian (40°S-10°S, 110°-155°E, land points only) temperature with SOI, and Australian precipitation with SOI are plotted for the model, along with the IPO index. The correlation time series are smoothed with a 13 year running mean, in order to highlight the interdecadal periods.

Similar relationships to the observations are found throughout most of the 300 year period of the model run. The correlations are consistently of the same sign (positive for Australian precipitation/SOI, negative for Australian temperature/SOI time series, which was multiplied by -1 in Fig. 5a, b), except for a few short periods. Strong correlations are typically found during negative IPO periods with weak correlations during positive IPO periods, although this relationship is not as consistent as that found in the observations with an overall correlation of the time series of IPO and Australian rainfall/SOI correlations of only -0.3 compared to a correlation of -0.8 in the observations.

There are some notable periods in the 300 year model run where the IPO and correlations are actually in phase (e.g., model years 180-210 where a drop in interannual correlations occur with negative IPO). This is an intriguing result as it raises the question of whether the observed relationship, calculated over less than 100 years, would undergo a similar shift in phase if a longer time series was available. This highlights the danger of trying to infer statistical cause and effect relations from relatively short observed records. However, it is also possible that this result is simply an artifact of the coupled model not simulating the climate system in a perfect manner. For the periods where the observed relationship does hold, we use the model as a tool to examine possible reasons for the interdecadal modulation of these interannual teleconnections.

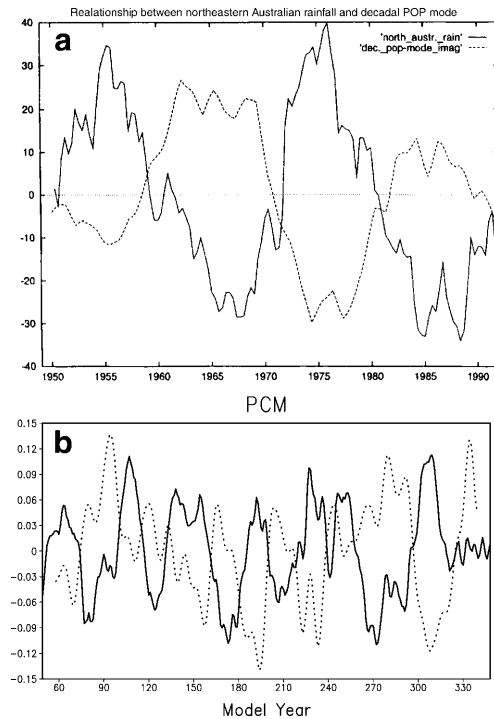


Fig. 4a, b Low pass filtered annual Australian rainfall and IPO index, observed (top) and model (bottom)

4.4 IPO mean climate changes

To compare mean climate states between positive and negative interdecadal periods in the PCM, a compositing technique was developed. Using the time series of Fig. 5, periods were chosen if they satisfied two criteria: (1) the IPO stayed the same sign (positive or negative) for at least 10 years running and was greater than ± 0.5 standard deviations and (2) the correlations of SOI and Australian precipitation were greater than 0.5 if the IPO was negative and the correlations were less than 0.5 if the IPO was positive. This criteria follows the observed relationship found by Power et al. (1999a) and shown in Fig. 5a. Since we want to use the model as a tool to study the observations, this technique restricts the composite periods to times when the model exhibits close to observed relationships.

In Fig. 6a, the PCM annual mean surface temperature for the positive minus negative composites is shown. As would be expected and as a test of the composite technique, the pattern is similar to that of the interdecadal mode of Fig. 3 with the pattern of warming in the tropical Pacific and cooling in the northwest and southwest Pacific regions. Temperatures over Australia are noticeably warmer during positive interdecadal periods, compared to negative interdecadal periods. The positive minus negative interdecadal composite for precipitation is given in Fig. 6b. Note that the entire Australian continent is drier, consistent with Fig. 4. These model results are also consistent with the observations, as shown in Power et al. (1999b).

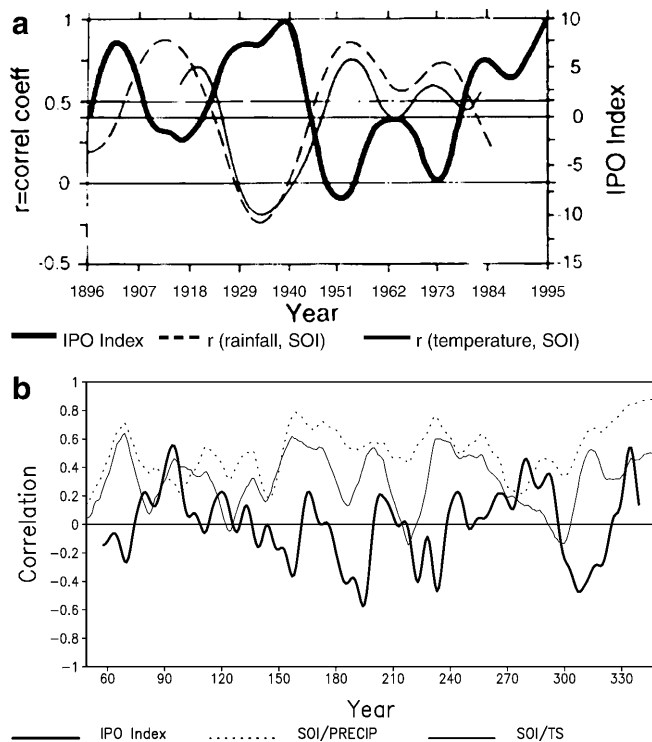


Fig. 5 Interdecadal modulation of interannual relationships between ENSO and Australian climate indices for observations (**a**; kindly reproduced from Power et al. 1999a) and **b** PCM. Correlations between SOI and surface temperature and SOI and precipitation were computed in 13 year running means. The IPO index for the model is taken from Fig. 1

5 Interdecadal modulation

We examine three possible mechanisms to explain the observed interdecadal modulation of the impact of ENSO on Australian climate. Recall that in the observations, interdecadal periods of warm SST anomalies in the tropical Pacific (positive IPO) are associated with a breakdown of the interannual teleconnection between ENSO and Australian rainfall. During these periods the positive IPO could be directly modulating ENSO, such that ENSO would have lower amplitude (due to a deeper thermocline; see next section) and thus a reduced interannual forcing on Australian rainfall. The IPO could also be changing the characteristics of the large scale east-west (or Walker) circulation which communicates changes in the eastern tropical Pacific to Australia. An eastward or westward shift of the rising branch of this circulation, usually centered over the maritime continent, would disrupt the direct interannual links between the tropical eastern Pacific and Australia.

5.1 Interdecadal modulation of ENSO

The first mechanism involves a direct modulation of the characteristics of ENSO. This could include changes to the frequency, seasonality, spatial patterns, intensity and

three-dimension structure of El Niño and La Niña events.

To examine how the structure of ENSO changes on interdecadal time scales, the long-term mean vertical cross section of Pacific ocean annual temperatures is shown in Fig. 7, along with the corresponding figure from the Levitus (1982) observational dataset. The PCM captures the observed east-west thermocline structure with a deeper thermocline in the western Pacific and shallower in the east. Although PCM is a few degrees colder than the observations, it has a close to observed vertical gradient in temperature in the top 400 m *i.e.*, a realistic thermocline structure. Recent studies, *e.g.*, Meehl et al. (2001) and Timmermann et al. (1999) have shown that this sharp thermocline is necessary for realistic ENSO variability in coupled models.

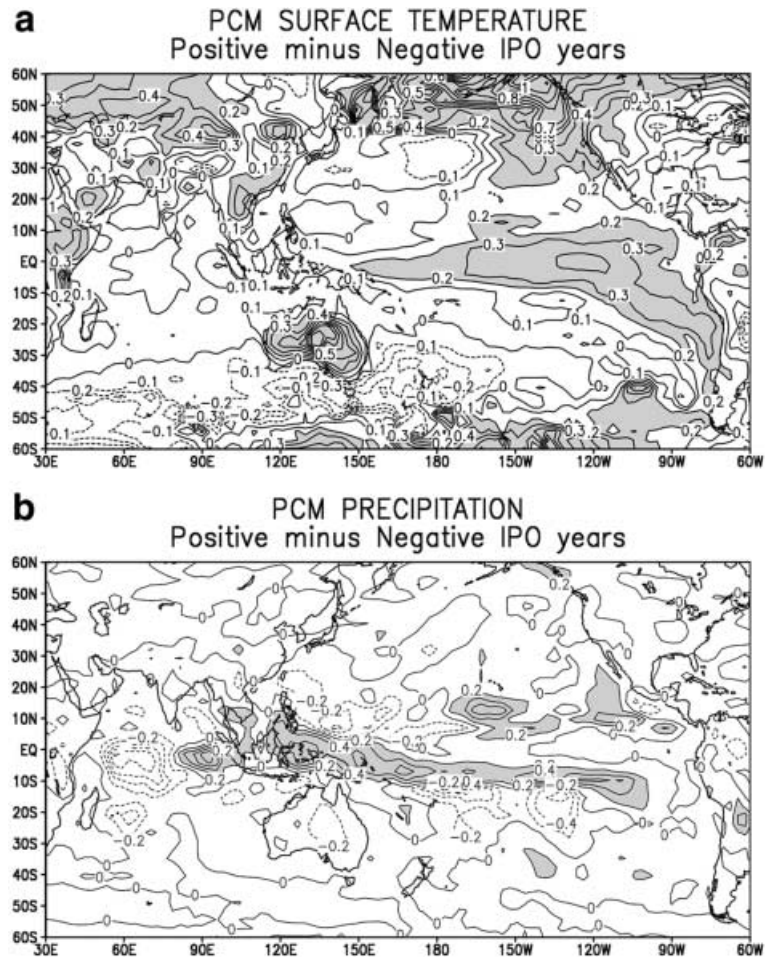
It has been shown that a deeper thermocline in the eastern Pacific (Niño-3 region) makes it more difficult for deeper waters to be upwelled, leading to lower amplitude ENSO variability since changes to the thermocline due to ocean dynamics would have less impact on the surface temperatures (*e.g.*, Pierce et al. 2000; Meehl et al. 2001). Figure 8 shows the positive minus negative IPO composites of the top 600 m of equatorial Pacific Ocean temperatures. The largest changes are found in the thermocline region (~ 175 m deep in the western Pacific and 100 m deep in the central to eastern Pacific) with a shallowing in the west and a deepening in the east. Though these changes are occurring on interdecadal time scales this is similar to what happens during an El Niño event with a corresponding slackening of the east-west temperature gradient. This is also consistent with changes in wind stress from positive to negative interdecadal periods in this region (not shown).

It would be expected from these changes in thermocline slope, that lower ENSO variability would be found during positive interdecadal periods due to the deepening of the thermocline in the eastern Pacific. This was investigated by calculating the standard deviation of Niño-3 (area average over 150°W - 90°W , 5°S - 5°N) and Niño-4 (area average over 160°E - 150°W , 5°S - 5°N) annual SSTs for the positive and negative composites. The results are shown in Table 1. As hypothesized, ENSO variance diminishes during positive interdecadal periods to 0.48°C compared to 0.65°C for the entire time series. This change from “normal” conditions is significant (using an *f*-test) at the 95 percentile. The changes in negative periods are not found to be significant. Similar changes are found for the Niño-4 SSTs. Hence, interdecadal variability in the PCM does modulate ENSO.

5.2 Interdecadal modulation of the Walker circulation

The second mechanism proposed was that the interdecadal oscillation modulates the way in which the effects of ENSO are communicated to Australia. Since ENSO is largely communicated to Australia via the Walker circulation, changes in this circulation, *e.g.*, its

Fig. 6 **a** Annual mean surface temperature (K) for positive minus negative interdecadal composites; **b** annual mean precipitation (mm/day) for positive minus negative interdecadal composites. Values greater than +0.2 are shaded



location or intensity, would be likely to affect how interannual variability associated with ENSO would influence Australian climate.

Kumar et al. (1999) looked at changes in the Walker circulation between 1958–1980 and 1981–1996. They found a southeastward shift of the rising branch of the Walker circulation during El Niño events in the more recent period and argue that this shift has led to the weakened relationship between the Indian monsoon and ENSO. Kumar et al. (1999) note that this shift could be due to global warming, however it could also be due to natural variability on interdecadal time scales.

Velocity potential, a measure of divergent flow, is often used as a proxy for the Walker circulation. The long term annual mean 200 hPa velocity potential for the PCM is given in Fig. 9a. Negative values indicate rising motion and positive values sinking motion. The Walker circulation of the Pacific is seen as rising motion over the western Pacific, Indonesia and northern Australia and sinking motion over the Americas and Africa.

To test changes in the Walker circulation on interdecadal time scales in the model, velocity potential was computed for the positive and negative interdecadal composite periods. Anomalies from the long term mean are shown in Fig. 9b and c. The positive composite anomalies indicate that the center of rising motion has

shifted east into the central Pacific, away from Australia, since there is anomalous rising there. During negative interdecadal periods (Fig. 9c) the center of action shifts in the opposite direction.

Hence, it appears that shifts in the Walker circulation occur on the interdecadal timescale such that the rising branch is further away from Australia during positive interdecadal tropical SST periods and could therefore contribute to ENSO's weaker influence on Australian rainfall during these periods.

5.3 Influence of western Pacific SSTs

As noted in Sect. 4, the warming of the tropical Pacific SSTs in the positive phase of the interdecadal mode extends further west than that of the ENSO mode (*e.g.*, Zhang et al. 1997). Although the model and observations differ somewhat in the eastern Pacific, they both exhibit more warming in the western Pacific in the interdecadal mode, relative to ENSO. Hence, sensitivity experiments were designed to try and isolate this difference and determine its impact on Australian climate. Presumably warm decadal SSTs in the western Pacific could have the effect of suppressing Australian rainfall and thus interfere with the teleconnections between

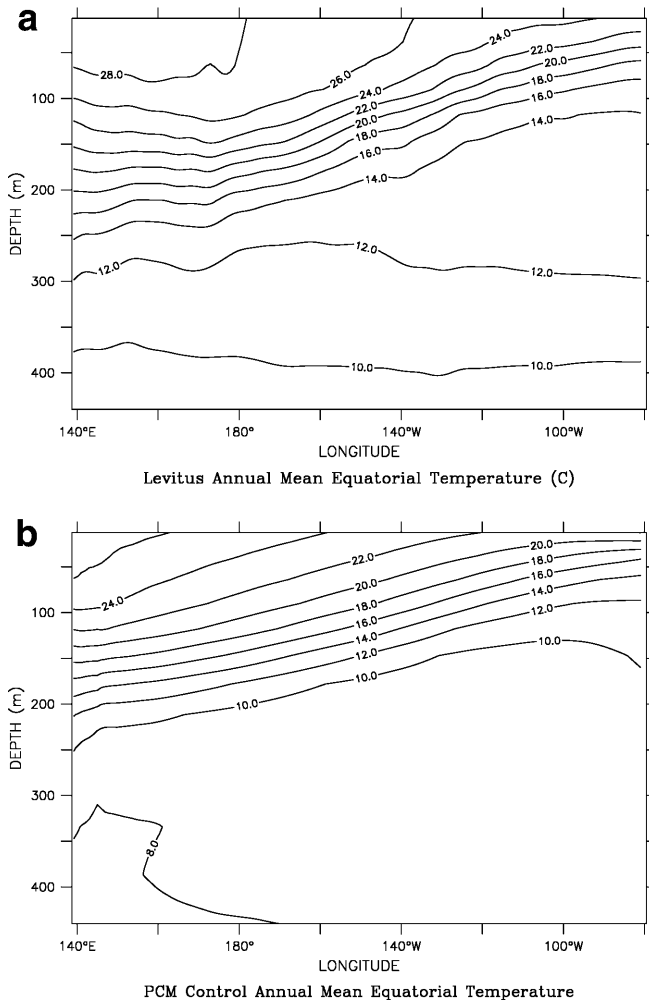


Fig. 7 **a** Levitus observations of annual mean ocean equatorial temperature in the Pacific sector and **b** corresponding cross section for the PCM

ENSO timescale SSTs further east, and vice versa for the cold experiment.

Two sensitivity experiments were run. Both were Atmospheric Model Intercomparison Project (AMIP) type experiments using the CCM3 atmospheric model forced with observed SSTs and sea-ice concentrations from 1979-1995. Recently an experiment of this type was run for the purposes of submission to the AMIP2 intercomparison project. Using the identical model code, SSTs in the western Pacific were perturbed, using the AMIP2 simulation as a control.

In the first sensitivity experiment, warm anomalies of 0.5 °C were added to the monthly SSTs in the western Pacific from 110°-180°E, 6°S-6°N. The second experiment was identical except 0.5 °C cold anomalies were added to the SSTs. Hence, the warm anomaly experiment was designed to represent positive interdecadal periods and the cold anomaly experiment, negative interdecadal periods. If decadal changes in the western Pacific SSTs are driving the interdecadal modulation of Australian climate, then drier conditions over Australia

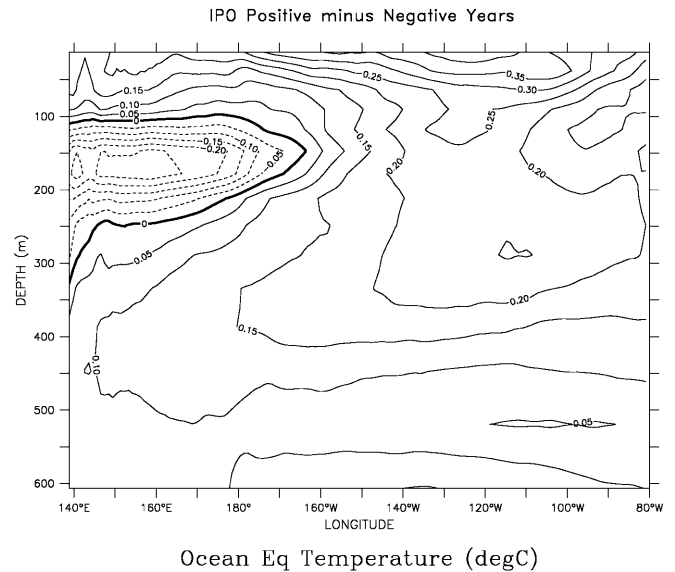


Fig. 8 PCM ocean cross-section of equatorial ocean temperature in the Pacific sector for positive minus negative interdecadal periods

Table 1 Niño-3 & 4 SST standard deviations for positive and negative IPO periods

	Standard deviations	
	Niño-3 SST	Niño-4 SST
All years	0.65	0.50
Positive IPO	0.48	0.42
Negative IPO	0.70	0.55

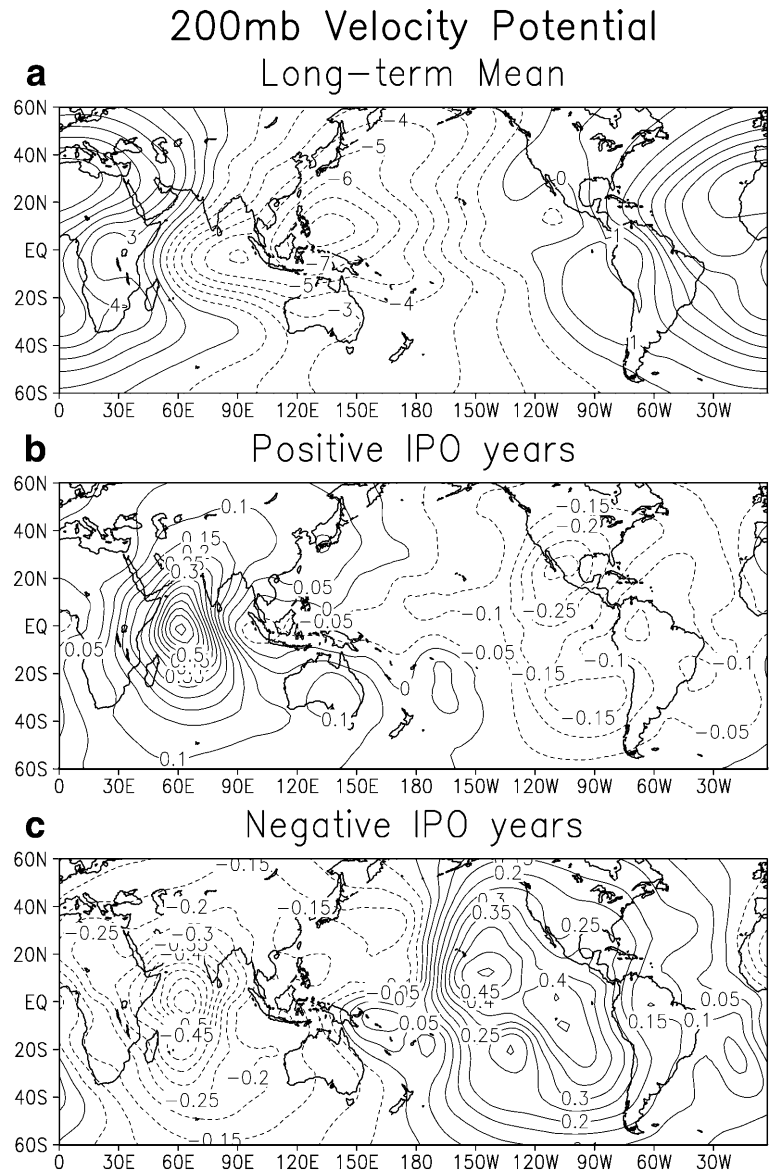
would be expected in the warm perturbation case and wetter conditions in the cold perturbation case (as in Fig. 4).

The key result from these experiments is shown in Fig. 10, the time series' of annual Australian precipitation for the control (AMIP2, solid line), western Pacific warm SST experiment (dashed) and western Pacific cold SST experiment (dotted). As hypothesized, the warm case results in drier conditions over the Australian continent. This is further demonstrated by the geographical pattern of changes in precipitation over Australia for the warm experiment anomalies, shown in Fig. 11. An anomalous regional Hadley circulation is set up over the warm SSTs with increased rising motion over the perturbed region and increased subsidence over Australia.

The cold case in Fig. 10 is slightly wetter than the control but the difference is not as dramatic as that for the warm experiment. Increasing temperatures in the western Pacific are expected to induce greater circulation changes than cooling them down by virtue of the Clausius-Clapeyron relation, that describes the nonlinear relationship between surface temperature and evaporation (Curry and Webster 1999).

Figure 10 demonstrates how the mean Australia rainfall is affected by these SST anomalies, but are the

Fig. 9 a Annual mean 200 hPa velocity potential for a long term mean. *Negative* contours indicate rising motion, *positive* contours indicate sinking motion. Units are $10^6 \text{ m}^2 \text{ s}^{-1}$. Anomalies from the long term mean are shown for **b** positive interdecadal periods and **c** negative interdecadal periods



ENSO teleconnections also affected? Since a time series of 16 years is quite short to determine this, an additional pair of warm and cold simulations were run. These were identical to the original sensitivity experiments except for initial conditions. Mean rainfall changes from these additional runs were similar to Fig. 10.

Correlations between Niño-3 SSTs and northeast Australian rainfall from both sets of experiments are given in Table 2. Northeast Australian rainfall was used in place of the all-Australian rainfall time series since the atmospheric model had a more realistic relationship with ENSO for the former region. Note that both warm and cold experiments show a slight weakening of the relationship between ENSO and Australian climate. That is, the negative correlation in the experiment 1 control run of -0.57 (signifying warm El Niño events in the Pacific are associated with suppressed northern Australian rainfall) drops somewhat to -0.47 and -0.44 for the warm and cold western Pacific SST experiments,

respectively. A similar but less strong weakening is seen in experiment 2, where the correlation of the control drops slightly to -0.62 and -0.61 in the warm and cold experiments, respectively. Hence the western Pacific does not appear to be the dominant influence on the relationship found in Fig. 5 [*i.e.*, the weakening of interannual correlations during positive (warm tropical Pacific SSTs) interdecadal periods and the strengthening during negative (cold tropical Pacific SSTs) interdecadal periods] since the correlations weaken for both the warm and the cold experiments.

The correlations from the control runs and the sensitivity experiments are all significant at the 10% level (using a *t*-test) so one interpretation of this result could be that the western Pacific SSTs act to modulate the mean interdecadal Australian rainfall, as seen in Fig. 10, but do not disrupt the interannual teleconnections substantially. Another conclusion could be that, since the correlations decrease in both experi-

ments, the western Pacific disrupts or overrides the influence of ENSO on Australian climate if its base state is perturbed in either direction, either warm or cold. Additional ensemble members would be required to explore this further. In any case, the model experiments indicate that the interdecadal modulation of interannual teleconnections (such that warm IPO periods have reduced interannual teleconnections between ENSO and Australian rainfall and cold periods enhance the interannual teleconnections) cannot be readily attributed to western Pacific SSTs in the model sensitivity experiments.

Note that the anomalies added (0.5 °C) in the model experiments are larger than the observed SST changes in the western Pacific in Fig. 6 (~0.2 °C). Larger anomalies were added in order to yield a statistically significant change in the circulation over the AMIP period. Ideally, further sensitivity experiments would be run, varying the size of the anomalies added, however, the expense of computer simulations restricts this.

6 Conclusions

Interdecadal variations in rainfall over the Australian continent were investigated in the PCM, a fully coupled climate model. Changes in interannual teleconnections

i.e., ENSOs influence on Australia, were examined in the context of positive and negative interdecadal periods.

An IPO index was defined as the principal component time series of the first EOF of lowpass filtered seasonal SSTs and was found to be anticorrelated with lowpass filtered Australian rainfall, similar to observed. Interannual model correlations between Australian climate and the SOI were computed in 13 year running blocks, similar to the observational study of Power et al. (1999a). Some periods of the model run exhibited characteristics similar to the observations with the IPO in opposite phase to that of the interannual correlations. Hence, the model captured the observed relationships found by Power et al. (1999a) whereby positive (warm tropical Pacific SSTs) interdecadal periods induced weak interannual teleconnections and negative (cold tropical Pacific SSTs) interdecadal periods coincided with strong interannual teleconnections. The PCM also showed periods where the IPO was in phase with the correlations suggesting that either the model is not consistently capturing the observed teleconnections, or the limited period of observations samples only a strong period of interdecadal teleconnectivity.

During positive interdecadal periods, the model was shown to have lower Niño-3 SST variance and a more relaxed thermocline. This supports the findings of Pierce et al. (2000) that observed El Nino amplitude is diminished during positive interdecadal periods, possibly leading to a weaker influence on Australian climate. This is also consistent with Power et al. (1999a) who found that, during the twentieth century, the variance of the SOI is approximately halved during positive phases of the IPO.

The rising branch of the Walker circulation in the model was found to shift eastward during these warm interdecadal periods, also contributing to a diminished

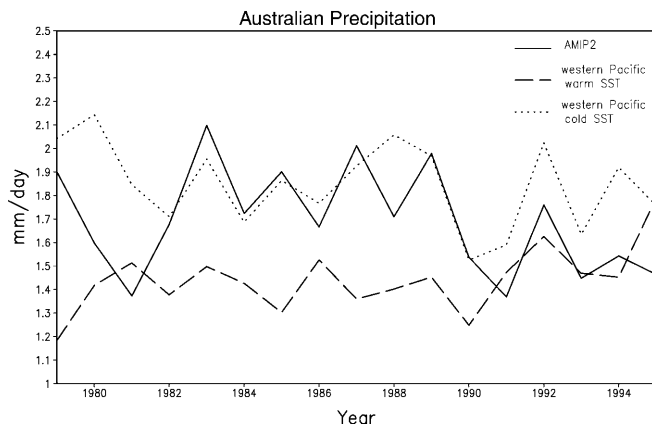


Fig. 10 Australian annual precipitation for the control (*solid*), warm perturbation sensitivity experiment (*dashed*) and cold perturbation (*dotted*)

Fig. 11 Precipitation (mm/day) for the DJF season over the Australasian region for the AMIP2_WP (warm western Pacific) experiment minus control. Values above +0.4 mm/day are shaded

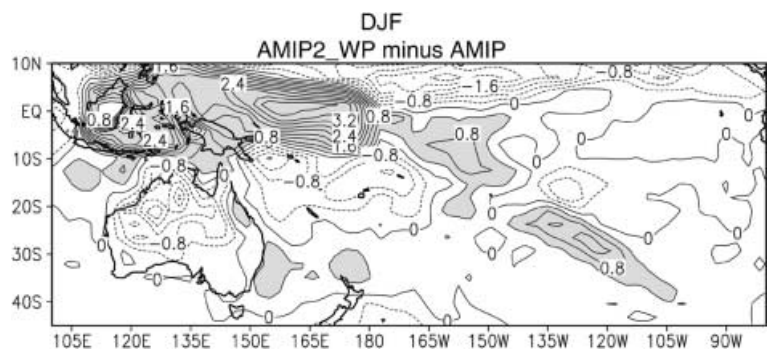


Table 2 Interannual correlations between Niño-3 SST and NE Australian annual rainfall from model experiments

Correlations	Experiment 1	Experiment 2
Control	-0.57	-0.67
Warm experiment	-0.47	-0.62
Cold experiment	-0.44	-0.61

influence of eastern Pacific interannual variations on Australian climate.

Sensitivity experiments with an atmospheric model were run to examine the influence of warm SSTs in the western Pacific on Australian rainfall, a characteristic of positive interdecadal periods but not El Niño. Warm western Pacific SSTs were found to draw the convection further north and hence contribute to decreased rainfall over the Australian continent. However, interannual correlations between ENSO and Australian rainfall did not change significantly when western Pacific SSTs were perturbed. Further sensitivity experiments are planned to examine these relationships.

Acknowledgement The authors thank Peter Webster and Scott Power for their scientific input and Tony Craig, Gary Strand and Erik Kluzek for model consultation. A portion of this study was supported by the Office of Biological and Environmental Research, U.S. Department of Energy, as part of its Climate Change Prediction Program. The National Center for Atmospheric Research is sponsored by the National Science Foundation.

References

- AchutaRao K, Sperber KR and the CMIP modelling groups (2000) El Nino Southern Oscillation simulation in coupled GCMs, PCMDI Report 61, pp 46
- Battisti DS, Hirst AC (1989) Interannual variability in the tropical atmosphere/ocean system: Influence of the basic state, ocean geometry and nonlinearity. *J Atmos Sci* 46: 1687–1712
- Bonan GB (1998) The land surface climatology of the NCAR Land Surface Model Coupled to the NCAR Community Climate Model. *J Clim* 11: 1307–1326
- Boville B, Gent PR (1998) The NCAR Climate System Model, version one. *J Clim* 11: 1115–1130
- Bryan K (1984) Accelerating the convergence to equilibrium of ocean-climate models. *J Phys Oceanogr* 14: 666–673
- Bryan K, Cox MD (1967) A numerical investigation of the oceanic general circulation. *Tellus* 19: 54–80
- Curry JA, Webster PJ (1999) Thermodynamics of atmospheres and oceans, Academic Press, New York, 471pp
- Folland CK, Parker DE, Colman A, Washington R (1999) Large scale modes of ocean surface temperature since the late nineteenth century. In: Navarra A (ed) *Beyond El Nino: decade 1 and interdecade 1 climate variability*. Springer, Berlin Heidelberg New York, pp 73–102
- Gu D, Philander SGH (1997) Interdecadal climate fluctuations that depend on exchanges between the tropics and extratropics. *Science* 275: 805–807
- Hack JJ (1994) Parameterization of moist convection in the National Center for Atmospheric Research community climate model (CCM2). *J Geophys Res* 99: 5551–5568
- Kiehl JT, Hack JJ, Bonan GB, Boville BA, Williamson DL, Rasch PJ (1998) The National Center for Atmospheric Research Community Climate Model: CCM3. *J Clim* 11: 1131–1150
- Kumar KK, Rajagopalan B, Cane MA (1999) On the weakening relationship between the Indian monsoon and ENSO. *Science* 284: 2156–2159
- Latif M (1998) Dynamics of interdecadal variability in coupled ocean-atmosphere models. *J Clim* 11:602–624
- Latif M, Kleeman R, Eckert C (1997) Greenhouse warming, decadal variability, or El Niño? An attempt to understand the anomalous 1990s. *J Clim* 10: 2221–2239
- Levitus S (1982) Climatological Atlas of the World Ocean. NOAA Prof. Pap 13, US Government Printing Office, 173pp
- Lysne J, Chang P, Giese B (1997) Impact of the extratropical Pacific on equatorial variability. *Geophys Res Lett* 24: 2589–2592
- Arblaster et al.: Interdecadal modulation of Australian rainfall
- Ma C-C, Mechoso CR, Robertson AW, Arakawa A (1996) Peruvian stratus clouds and the tropical Pacific circulation: A coupled ocean-atmosphere GCM study. *J Clim* 9:1635–1645
- Mantua NJ, Hare SR, Zhang Y, Wallace JM, Francis RC (1997) A Pacific interdecadal climate oscillation with impacts on salmon production. *Bull Am Met Soc* 78:1069–1079
- McCreary JP (1983) A model of tropical ocean-atmosphere interaction. *Mon Weather Rev* 111: 370–387
- McCreary JP, Anderson DLT (1984) A simple model of El Niño and the Southern Oscillation. *J Geophys Res* 122: 934–946.
- McPhaden MJ (1999) Genesis and evolution of the 1997-98 El Niño. *Science* 283: 950–954
- McPhaden MJ and co-authors (1998) The Tropical Ocean-Global Atmosphere observing system: a decade of progress. *J Geophys Res* 103: 14169–14240
- Meehl GA, Arblaster JM (1998) The Asian-Australian monsoon and El Niño-Southern Oscillation in the NCAR Climate System Model. *J Clim* 11: 1356–1385
- Meehl GA, Arblaster JM, Strand Jnr WG (1998) Global scale decadal climate variability. *Geophys Res Lett* 25: 3983–3986
- Meehl GA, Gent PR, Arblaster JM, Otto-Bliesner BL, Brady EC, Craig AP (2001) Factors that affect amplitude of El Niño in global coupled climate models. *Clim Dyn* 7: 515–526
- Nicholls N, Lavery B, Frederiksen C, Drosowsky W, Torok S (1996) Recent apparent changes in relationships between the El Niño – southern oscillation and Australian rainfall and temperature. *Geophys Res Lett* 23: 3357–3360
- Pacanowski RC, Philander SGH (1981) Parameterization of vertical mixing in numerical models of the tropical oceans. *J Phys Oceanogr* 11: 1443–1451
- Pierce DW, Barnett TP, Latif M (2000) Connections between the Pacific ocean tropics and midlatitudes on decadal time scales. *J Clim* 13: 1173–1194
- Power S, Casey T, Folland C, Colman A, Mehta V (1999a) Interdecadal modulation of the impact of ENSO on Australia. *Clim Dyn* 15: 319–324
- Power S, Tseitkin F, Mehta V, Lavery B, Torok S, Holbrook N (1999b) Decadal climate variability in Australia during the twentieth century. *Intl J Climatol* 19: 169–184
- Reynolds RW, Smith TM (1994) Improved global sea temperature analyses using optimum interpolation. *J Clim* 7: 929–948
- Ropelewski CF, Halpert MS (1996) Quantifying Southern Oscillation-precipitation relationships. *J Clim* 9: 1043–1059
- Semtner AJ (1995) Modeling ocean circulation. *Science* 269: 1379–1385
- Smith RD, Kortas S, Meltz B (1995) Curvilinear coordinates for global ocean models, LA-UR-95-1146, Los Alamos National Laboratory, Los Alamos, New Mexico, USA, 38pp
- Suarez MJ, Schopf PS (1988) A delayed action oscillator for ENSO. *J Atmos Sci* 45: 3283–3287
- Timmermann A, Oberhuber J, Bacher A, Esch M, Latif M, Roeckner E (1999) Increased El Niño frequency in a climate model forced by future greenhouse warming. *Nature* 398: 694–697
- Torrence C, Webster PJ (1999) Interdecadal changes in the ENSO-monsoon system. *J Clim* 12: 2679–2690
- Trenberth KE, Hurrell JW (1994) Decadal atmosphere-ocean variations in the Pacific. *Clim Dyn* 9: 303–319
- Trenberth KE (1997) The definition of El Niño. *Bull Am Meteorol Soc* 78: 2771–2777
- Walland DJ (1998) Seasonal climate summary southern hemisphere (spring 1997): a strong Pacific warm episode (El Niño) nears maturity. *Aust Meteorol Mag* 47: 159–166
- Washington WM and co-authors (2000) Parallel Climate Model (PCM) control and transient simulations. *Clim Dyn* 16: 755–774
- Webster PJ, Palmer TN (1997) The past and the future of El Niño. *Nature* 390: 562–564
- Webster PJ, Magana V, Palmer TN, Shukla J, Tomas RA, Yanai M, Yasunari T (1998) Monsoons: Processes, predictability and the prospects for prediction. *J Geophys Res* 103: 14451–14510
- Xie P, Arkin PA (1996) Analyses of global monthly precipitation using gauge observations, satellite estimates, and numerical model predictions. *J Clim* 9:840–858

- Zhang GJ, McFarlane NA (1995) Sensitivity of climate simulations to the parameterization of cumulus convection in the Canadian Climate Centre general circulation model. *Atmos-Ocean* 33: 407–446
- Zhang JL, Hibler III WD (1997) On an efficient numerical method for modeling sea ice dynamics. *J Geophys Res* 102: 8691–8702
- Zhang Y, Wallace JM, Battisti DS (1997) ENSO-like interdecadal variability: 1900-93. *J Clim* 10: 1004–1020